Revealing flow behaviors of metallic glass based on activation of flow units

T. P. Ge, W. H. Wang, and H. Y. Bai

Citation: Journal of Applied Physics **119**, 204905 (2016); doi: 10.1063/1.4952737
View online: http://dx.doi.org/10.1063/1.4952737
View Table of Contents: http://scitation.aip.org/content/aip/journal/jap/119/20?ver=pdfcov
Published by the AIP Publishing

Revealing flow behaviors of metallic glass based on activation of flow units

T. P. Ge, W. H. Wang, and H. Y. Bai[a)]
Institute of Physics, Chinese Academy of Sciences, Beijing 100190, People's Republic of China

(Received 22 March 2016; accepted 14 May 2016; published online 26 May 2016)

Atomic level flow plays a critical role in the mechanical behavior of metallic glass (MG) while the connection between the flow and the heterogeneous microstructure of the glass remains unclear. We describe the heterogeneity of MGs as the elastic matrix with "inclusions" of nano-scale liquid-like flow units, and the plastic flow behavior of MGs is considered to be accommodated by the flow units. We show that the model can explain the various deformation behaviors, the transformation from inhomogeneous deformation to homogeneous flow upon strain rate or temperature, and the deformation map in MGs, which might provide insights into the flow mechanisms in glasses and inspiration for improving the plasticity of MGs. *Published by AIP Publishing*.
[http://dx.doi.org/10.1063/1.4952737]

I. INTRODUCTION

Metallic glasses (MGs) have a unique mechanical performance such as high strength, high hardness, large elastic limit, and good wear resistance, which has potential functional and structural applications. Due to the liquid-like long-range disordered structure and the lack of defects of dislocations in crystalline solids, the flow of MGs is usually localized in nano-scaled regions of shear bands,[1–5] which leads to limited plastic flow or macroscopic brittle behavior. The inhomogeneously localized flow in MG can transform into the homogeneous flow at some conditions such as low strain rate or approaching the glass transition temperature (T_g),[6–8] which makes the MGs have the superplastic forming ability.[9,10] However, the mechanism of the flow behaviors as well as their relationship with the heterogeneous structure of the metallic glass remains unclear. Some models based on the mean field theory[11–21] have been proposed to understand the connection between the property and the flow deformation in MGs while these models cannot explain the relation between the property and its microscopic structure. Recently, the heterogeneity of MGs has been confirmed by experiments and simulations.[21–32] To characterize the structural heterogeneity, the flow units concept[18] is introduced to describe the structural heterogeneity and to explain the mechanical behaviors of MGs. The flow units are the liquid-like regions embedded in the elastic matrix of MGs with a lower activation energy and can be activated easily by temperature or stress,[6,33] which can carry the deformations, relaxations, rejuvenation, and mechanical and physical properties of MGs.[34–39]

In this article, we investigate the microscopic mechanism of flow deformation in a $La_{60}Ni_{15}Al_{25}$ metallic glass in the perspective of the flow unit concept. We describe the heterogeneity of MG with the flow unit model and consider the plastic flow of MG to be accommodated by these flow units. We show that the model can explain the different deformation behaviors of MG and build a deformation map to exhibit the transformation from inhomogeneous to homogeneous deformations upon strain rate or temperature.

II. EXPERIMENTAL

We used a $La_{60}Ni_{15}Al_{25}$ MG as a model system to investigate the flow in MGs. The alloys were prepared by arc melting the constituent elements with a purity of at least 99.9 at. % in a Ti-gettered argon atmosphere. The cylindrical samples of 2 mm in diameter were prepared by suck casting the ingots into a water-cooled copper mold. The amorphous structure was confirmed by X-ray diffraction (XRD) and differential scanning calorimetry (DSC). Samples for compression tests with 4 mm in length were cut from the rod, and the samples were initialized by using DSC to guarantee that all the samples were in the same initial state. The samples were heated up to 488 K and then cooled down to 313 K in the same rate of 20 K/min. The uniaxial compression was carried with different strain rates by using an electro-mechanical testing machine (Instron electromechanical 3384 test system) at 413 K ($\sim 0.9T_g$). The samples were kept at this temperature for 10 min before compression to make sure the temperature was stable.

III. RESULTS AND DISCUSSION

Figure 1 shows the engineering stress-strain (SS) curves of $La_{60}Ni_{15}Al_{25}$ at 413 K ($\sim 0.9T_g$) with different strain rates. One can see that the deformation behaviors of MGs are sensitively depended on the strain rate. If the strain rate is relatively high, the MG likes a spring and behaves elastically in its elastic region, and the applied stress is proportional to the strain. When the applied stress is larger than the yielding stress, the MG behaves macroscopically pure brittle and will fracture immediately after the elastic deformation (the black curve in Fig. 1). If the strain rate is relatively low, the MG will behave like Newtonian flow, which can be described by the Maxwell model: $\dot{\gamma} = \frac{\dot{\sigma}}{E} + \frac{\sigma}{\eta}$, where $\dot{\gamma}$ is the strain rate, $\dot{\sigma}$ is the stress rate, E is the Young's modulus, and η is the viscosity. For the appropriate strain rate, the behavior of the flow in MG is non-Newtonian, which shows both elastic behavior

a)Author to whom correspondence should be addressed. Electronic mail: hybai@iphy.ac.cn

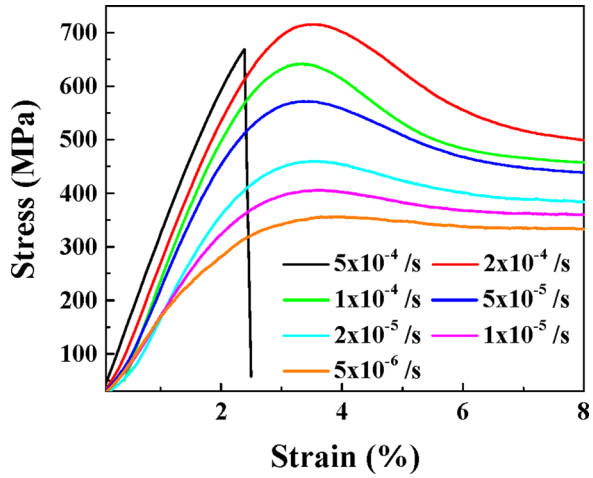

FIG. 1. The engineering stress strain curves of $La_{60}Ni_{15}Al_{25}$ metallic glass under strain rates of 5×10^{-4}, 2×10^{-4}, 1×10^{-4}, 5×10^{-5}, 2×10^{-5}, 1×10^{-5}, and $5 \times 10^{-6}\,s^{-1}$.

before yielding and plastic flow behavior after yielding. These different flow behaviors, presenting the change of the inherent structure of the glass, are hard to be explained by the mean field theory.

The MGs cannot be solely described using a Maxwell model due to the existence of both the elastic matrix and the liquid like regions or flow units in MGs.[26–39] So, the three-parameter viscoelastic model,[26,34] as shown in Fig. 2(a), is applied to explain the mechanical behaviors of the elastic matrix and the flow units during deformations of MGs. In the three-parameter viscoelastic model, the elastic matrix is represented by a spring with modulus E_1, and the flow unit is represented by the tandem of a spring and a dashpot with modulus E_2 and viscosity η, respectively. We assume that the MG consists of flow units with a fraction of c and then the concentration of elastic matrix is $(1–c)$. Thus, the total stress σ, which is assumed to be the sum of the accommodated stress of the elastic matrix σ_e and flow units σ_f, can be expressed as

$$\sigma = (1 - c)\sigma_e + c\sigma_f. \tag{1}$$

We applied Eq. (1) to describe the deformation behavior of MGs, which is assumed to be constituted of the elastic matrix and the flow units.

The previous investigations on the fractions of flow units and free volumes in metallic glasses show that the flow units and the free volumes have a strong connection, and there is a linear relationship between the concentration of the free volumes and the flow units in MGs.[40–42] The free volume defect concentration c_f can be described by the rate equation[40] $\frac{dc_f}{dt} = -k_r c_f (c_f - c_{f,eq})$, where t is the time, and k_r and $c_{f,eq}$ are the constants. We assume that the fraction of flow units c has a linear relation with c_f and can also be described with the rate equation

$$\frac{dc}{dt} = -k(c - c_0)(c - c_{max}), \tag{2}$$

where k is the rate constant depending on the activation energy, c_0 and c_{max} are the lower and upper limit of c, respectively. The SS curve of the elastic matrix follows

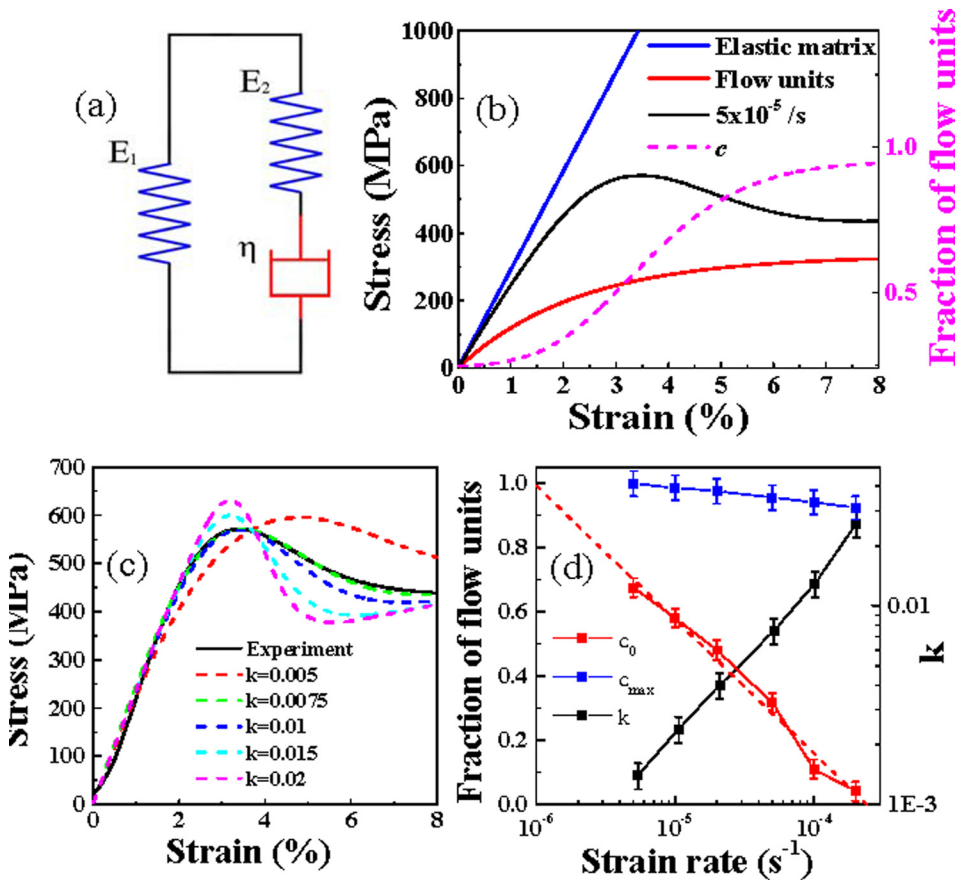

FIG. 2. (a) A sketch of the three parameters model, which described MG as a spring and a Maxwell model connected in parallel. (b) An example of the calculated SS curves of the elastic matrix (blue line), flow units (red line), and the $La_{60}Ni_{15}Al_{25}$ MG with a strain rate of 5×10^{-5}/s (the black line). The magenta dashed line is the fraction of flow units. (c) The calculated SS curves with different fitting values of k. The black solid line is the experimental SS curve with a strain rate of 5×10^{-5}/s. (d) The values of c_0, c_{max} and k at different strain rates. The dashed line is the linear fit of c_0. The solid lines are the guidelines for the eyes.

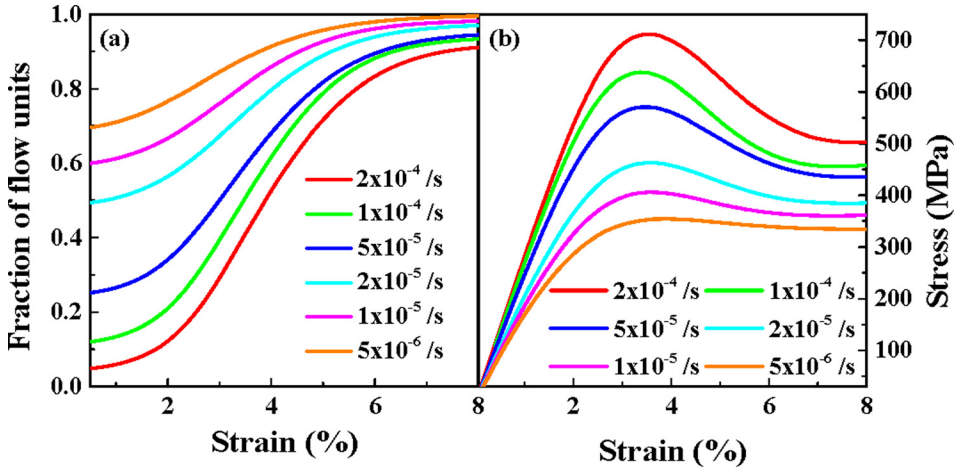

FIG. 3. (a) The calculated c vs. strain at different strain rates. (b) The calculated SS curves at different strain rates using Eq. (1).

$\sigma_e = \gamma E_1$, where γ is the strain and $E_1 = 29.2$ GPa, which is obtained from the SS curve with a strain rate of 5×10^{-4}/s [see the blue line in Fig. 2(b)]. For flow units, $\sigma_f = \sigma_s(1\text{-exp}(-E_2\gamma/\sigma_s))$, where $\sigma_s = 334.3$ MPa is the stable flow stress, and $E_2 = 14.71$ GPa, which are obtained from the SS curve with a strain rate of 5×10^{-6}/s [see the red line in Fig. 2(b)]. The dashed magenta curve in Fig. 2(b) is the evolution of c upon strain described by Eq. (2). Based on the curve of σ_e, σ_f, and c upon strain, we can fit the SS curves using Eq. (1) as the black curve shown in Fig. 2(b). The parameters in Eq. (2) are adjusted to make the best fit with the experiment SS curve. Figure 2(c) shows the calculated SS curves with different values of k in comparison with the experiment SS curve with a strain rate of 5×10^{-5}/s. Obviously, the fitting curve with $k = 0.0075$ fits best with the experiment SS curve. The other parameters c_0 and c_{max} are also determined. Thus, we can fit the SS curve at a strain rate of 5×10^{-5}/s using Eq. (1) and get the fitted c value, as shown in Fig. 2(b). When different strain rates are applied, the MGs show different deformation behaviors and display different values and evolution of c upon strain, and the parameters in Eq. (2) also change with the strain rate. Figure 2(d) shows the fitted values of these parameters under different strain rates. Using these parameters, we get the evolution curves of c upon strain under different strain rates as shown in Fig. 3(a), and the calculated SS curves of MGs using Eq. (1) under different strain rates.

As shown in Fig. 3(a), the fraction of flow unit c changes with strain rate, which determines the mechanical properties of MGs. The changing tendency of c upon strain rate is roughly consistent with the experimental results.[43–48] The corresponding calculated SS curves under different strain rates based on flow units model and Eq. (1) are shown in Fig. 3(b). Under a higher strain rate, the fraction of the activated flow units is smaller and the modulus and strength become higher according to Eq. (1). On the contrary, the lower strain rate can activate more flow units, and the MGs become more liquid-like with lower modulus and strength. When the strain rate is high enough, there are no activated flow units and c approaches zero,[6] and in this case, the MGs cannot flow and crack immediately after yielding. When the strain rate is low enough, there is no overshoot in the SS curve and the Newtonian flow happens. The calculated SS curves under different strain rates based on flow units model and Eq. (1) are in good accordance with experimental observation shown in Fig. 1, indicating that the flow unit model can well describe the deformation behaviors in MGs.

Based on Eq. (1), the c has a direct connection with the mechanical property of MGs, and the mechanical properties can be assumed as being contributed by both the elastic matrix and the flow units, and can be expressed as the combination effect of liquid-like regions of flow units and solid-like regions of the elastic matrix in a MG. For example, the Young's modulus, E, and the yielding strength, σ_y, both change with the fraction of flow units of c in MGs, can be regarded as the linear superposition of that of the elastic matrix and flow units with following linear relationship:

$$E = E_e(1 - c) + E_f c, \tag{3}$$

$$\sigma_y = \sigma_e(1 - c_y) + \sigma_f c_y, \tag{4}$$

where c_y is the fraction of flow units at the peak of the overshoot in SS curves. Figure 4 shows the relationship between Young's modulus, yielding strength, and c. The circle points in Fig. 4 display the experimental Young's modulus s under different strain rates evaluated with $E = \sigma/\gamma$, and the values

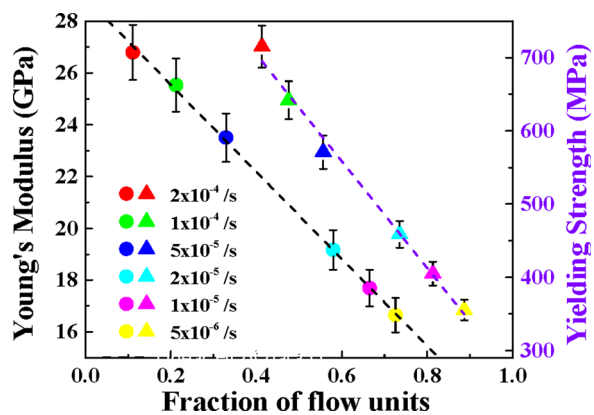

FIG. 4. The relationship between properties of MGs and the fraction of flow units. The circle points are Young's Modulus vs. the fraction of flow units at 1% strain and the triangle points are yielding strength vs. the fraction of flow units at the peak of the overshoot. The colors of these points show their corresponding strain rates. The dashed lines are the linear fits of these points.

of stress σ and strain γ are obtained from the points with 1% strain in the SS curves. The triangle points showing the experimental yielding strengths under different strain rates are the stress at the peak of the overshoot in these SS curves. One can see that both the E and σ_y of the MG show a linear relationship with the fraction of the flow units and can be well fitted using Eqs. (3) and (4), indicating that our flow unit model can describe the mechanical properties of strength and elastic modulus of MGs.

The flow unit model can also be used to describe the deformation map in MGs. Under relative high strain rate, the MG behaves inhomogeneous deformation due to the value of c approaches zero in the elastic region. That is, c_0, the lower limit of c, should be zero. Under very low strain rates, the MG shows Newtonian flow, and c and c_0 approach one. The linear fit of the relationship between c_0 and strain rate in Fig. 2(d) can be used to evaluate the critical strain rates. When $c_0 = 0$, the corresponding strain rate is 2.4×10^{-4}/s, which is the critical strain rate between inhomogeneous deformation and homogeneous flow. When $c_0 = 1$, the corresponding strain rate is 10^{-6}/s, which is the critical strain rate between non-Newtonian flow and Newtonian flow. At appropriate strain rates, the non-Newtonian flow happens, where the elastic matrix changes to flow units gradually. The deformation behavior evolution of MG is actually determined by the amount of the flow units activated by strain or temperature, which well correspond to the experimental deformation or flow map.

IV. CONCLUSION

The MGs can be simplified to be the elastic matrix with "inclusions" of liquid-like flow units, and the deformation of MGs can be treated as the combination of elastic deformation of the matrix and liquid-like flow of flow units. The flow unit concept can explain the deformation behaviors of MGs including the transformation from inhomogeneous deformation to homogeneous flow upon strain rate or temperature, and the deformation map. This work assists in understanding the deformations in MGs and may also give some inspirations in improving the plasticity of MGs.

ACKNOWLEDGMENTS

We are thankful for the experimental assistant and discussions from C. Wang, D. Q. Zhao, and D. W. Ding. This work was supported by the NSF of China (Grant No. 51271195) and MOST 973 Program (No. 2015CB856803).

[1]C. A. Pampillo, J. Mater. Sci. **10**, 1194 (1975).
[2]J. Schroers and W. L. Johnson, Phys. Rev. Lett. **93**, 255506 (2004).
[3]X. K. Xi, D. Q. Zhao, M. X. Pan, W. H. Wang, Y. Wu, and J. J. Lewandowski, Phys. Rev. Lett. **94**, 125510 (2005).
[4]J. J. Lewandowski and A. L. Greer, Nat. Mater. **5**, 15 (2006).
[5]A. L. Greer, Y. Q. Cheng, and E. Ma, Mater. Sci. Eng. R **74**, 71 (2013).
[6]T. P. Ge, X. Q. Gao, B. Huang, W. H. Wang, and H. Y. Bai, Intermetallics **67**, 47 (2015).
[7]J. Lu, G. Ravichandran, and W. L. Johnson, Acta Mater. **51**, 3429 (2003).
[8]P. F. Guan, M. W. Chen, and T. Egami, Phys. Rev. Lett. **104**, 205701 (2010).
[9]J. Ma, L. S. Huo, D. Q. Zhao, and W. H. Wang, J. Appl. Phys. **113**, 104505 (2013).
[10]J. Schroers, JOM **57**, 35 (2005).
[11]Y. Tong, T. Iwashita, W. Dmowski, H. Bei, Y. Yokoyama, and T. Egami, Acta Mater. **86**, 240 (2015).
[12]J. S. Harmon, M. D. Demetriou, W. L. Johnson, and K. Samwer, Phys. Rev. Lett. **99**, 135502 (2007).
[13]W. Dmowski, Y. Tong, T. Iwashita, Y. Yokoyama, and T. Egami, Phys. Rev. B **91**, 060101 (2015).
[14]R. Zallen, Am. J. Phys. **54**, 862 (1986).
[15]F. H. Stillinger and P. G. Debenedetti, Annu. Rev. Condens. Matter. Phys. **4**, 263 (2013).
[16]F. Spaepen, Acta Metall. **25**, 407 (1977).
[17]F. Spaepen and D. Turnbull, Scr. Metall. **8**, 563 (1974).
[18]A. S. Argon, Acta Metall. **27**, 47 (1979).
[19]W. Johnson and K. Samwer, Phys. Rev. Lett. **95**, 195501 (2005).
[20]M. Zhang, L. Liu, and Y. Wu, J. Chem. Phys. **139**, 164508 (2013).
[21]A. Tanguy, J. Wittmer, F. Leonforte, and J. L. Barrat, Phys. Rev. B **66**, 174205 (2002).
[22]Y. Yang, J. F. Zeng, J. C. Ye, and J. Lu, Appl. Phys. Lett. **97**, 261905 (2010).
[23]W. Dmowski, T. Iwashita, C. P. Chuang, J. Almer, and T. Egami, Phys. Rev. Lett. **105**, 205502 (2010).
[24]Y. Cheng and E. Ma, Phys. Rev. B **80**, 064104 (2009).
[25]Y. H. Liu, D. Wang, K. Nakajima, W. Zhang, A. Hirata, T. Nishi, A. Inoue, and M. W. Chen, Phys. Rev. Lett. **106**, 125504 (2011).
[26]L. S. Huo, J. F. Zeng, W. H. Wang, C. T. Liu, and Y. Yang, Acta Mater. **61**, 4329 (2013).
[27]Y. Yang, J. F. Zeng, A. Volland, J. J. Blandin, S. Gravier, and C. T. Liu, Acta Mater. **60**, 5260 (2012).
[28]S. V. Khonik, A. V. Granato, D. M. Joncich, A. Pompe, and V. A. Khonik, Phys. Rev. Lett. **100**, 065501 (2008).
[29]Y. Fan, T. Iwashita, and T. Egami, Phys. Rev. E **89**, 062313 (2014).
[30]W. Schirmacher, G. Ruocco, and V. Mazzone, Phys. Rev. Lett. **115**, 015901 (2015).
[31]Y. Fan, T. Iwashita, and T. Egami, Nat. Commun. **5**, 5083 (2014).
[32]E. D. Cubuk, S. S. Schoenholz, J. M. Rieser, B. D. Malone, J. Rottler, D. J. Durian, E. Kaxiras, and A. J. Liu, Phys. Rev. Lett. **114**, 108001 (2015).
[33]Y. J. Wang, M. Zhang, L. Liu, S. Ogata, and L. H. Dai, Phys. Rev. B **92**, 174118 (2015).
[34]L. S. Huo, J. Ma, H. B. Ke, H. Y. Bai, D. Q. Zhao, and W. H. Wang, J. Appl. Phys. **111**, 113522 (2012).
[35]Z. Wang, P. Wen, L. S. Huo, H. Y. Bai, and W. H. Wang, Appl. Phys. Lett. **101**, 121906 (2012).
[36]W. Jiao, B. A. Sun, P. Wen, H. Y. Bai, Q. P. Kong, and W. H. Wang, Appl. Phys. Lett. **103**, 081904 (2013).
[37]S. T. Liu, W. Jiao, B. A. Sun, and W. H. Wang, J. Non-Cryst. Solids **376**, 76 (2013).
[38]D. P. Wang, Z. G. Zhu, R. J. Xue, D. W. Ding, H. Y. Bai, and W. H. Wang, J. Appl. Phys. **114**, 173505 (2013).
[39]Z. G. Zhu, P. Wen, D. P. Wang, R. J. Xue, D. Q. Zhao, and W. H. Wang, J. Appl. Phys. **114**, 083512 (2013).
[40]P. de Hey, J. Sietsma, and A. van den Beukel, Acta Mater. **46**, 5873 (1998).
[41]S. S. Tsao and F. Spaepen, Acta Metall. **33**, 881 (1985).
[42]L. Z. Zhao, R. J. Xue, Z. G. Zhu, Z. Lu, E. Axinte, W. H. Wang, and H. Y. Bai, J. Appl. Phys. **116**, 103516 (2014).
[43]R. J. Xue, D. P. Wang, Z. G. Zhu, D. W. Ding, B. Zhang, and W. H. Wang, J. Appl. Phys. **114**, 123514 (2013).
[44]L. Z. Zhao, R. J. Xue, Y. Z. Li, W. H. Wang, and H. Y. Bai, J. Appl. Phys. **118**, 244901 (2015).
[45]Z. Wang, B. A. Sun, H. Y. Bai, and W. H. Wang, Nat. Commun. **5**, 5823 (2014).
[46]X. F. Cao, M. Gao, L. Z. Zhao, W. H. Wang, and H. Y. Bai, J. Appl. Phys. **119**, 084906 (2016).
[47]W. H. Wang, Y. Yang, T. G. Nieh, and C. T. Liu, Intermetallics **67**, 81 (2015).
[48]W. Jiao, P. Wen, H. L. Peng, H. Y. Bai, B. A. Sun, and W. H. Wang, Appl. Phys. Lett. **102**, 101903 (2013).